Optical Materials 112 (2021) 110695

Contents lists available at ScienceDirect

Optical Materials

journal homepage: http://www.elsevier.com/locate/optmat

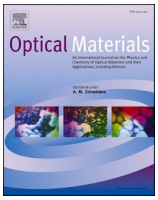

Nonlinear optical properties and markedly higher two photon absorption of ordered c-shaped plasmon-active metal nanostructures

J. Švanda [a,b,*], Y. Kalachyova [b], A. Ajami [c,d], W. Husinsky [d], P. Macháč [b], J. Siegel [b], Z. Kolská [e], P. Slepička [b], V. Švorčík [b], O. Lyutakov [b]

[a] Baumit, Spol. S.r.o., 250 01, Brandýs Nad Labem, Czech Republic
[b] Department of Solid State Engineering, University of Chemistry and Technology, 16628, Prague, Czech Republic
[c] Faculty of Physics, Semman University, P. O. Box 35195-363, Semman, Iran
[d] Institute of Applied Physics, Vienna University of Technology, 1040, Vienna, Austria
[e] Faculty of Science, J. E. Purkyne University, 40096, Usti Nad Labem, Czech Republic

A B S T R A C T

Development of materials with highly nonlinear optical activity represents an intensively studied discipline due to potentially unique applications of such materials in photonics and information technologies. In this work the creation of ordered nanostructured arrays of c-shaped metals (Ag, Au, Al, and Pd) and characterization of their nonlinear optical properties are described. Large scale ordered arrays were created by the excimer laser pattering of a polymer surface and subsequent coating with Ag, Au, Al, and Pd. The successful creation of required structures was confirmed by the conductive AFM and FIB-SEM techniques. Linear optical response of the structures was examined using the UV–Vis technique and strong excitation of surface plasmon polariton resulting in appearance of strong absorption band was confirmed. The Z-scan technique with femtosecond laser pulses was used to determine the nonlinear optical response of the prepared metal arrays. It was found that the strong two-photon absorption appears under the illumination at the wavelength corresponding to the surface plasmon excitation. Extensive comparison with available literature data shows that the present structures exhibit markedly higher two-photon absorption activity.

1. Introduction

Nowadays, nonlinear optics (NLO) are of a great interest because of the great number of their potential applications in high-speed optical signal processing, ultrafast switching, ultra short pulse generation, second-harmonic generation etc. [1–5] NLO processes, governed by photon-photon interactions in suitable materials, include a broad spectrum of phenomena such as optical frequency conversion, phase conjugation, Kerr effect, two-photon absorption, Raman scattering, and so on [6]. All materials can potentially show the NLO behavior but in practice, the weak nature of optical nonlinearities requires the high light intensity, which can damage materials before the optical nonlinearities reach a reasonable level [7,8].

However, there is an elegant way how to boost NLO effects without the materials damage, i.e. using of the spatial concentration of light in plasmonic nanostructures. The distinctive ability of plasmonic structures to concentrate light energy in deep sub-wavelength space is actually used in the fields of ultrasensitive sensors and ultrafast optical modulation [9,10]. This also provides an efficient pathways to decrease light intensity required for NLO phenomena induction [11]. In other words, strong light localization significantly facilitates NLO effects [12,13]. Moreover, plasmon-based NLO structures can combine the NLO effects enhancement typical for noble metals with ultrafast optical response times and allow NLO components to be scaled down in size [13]. Additionally, the plasmonic nanostructures offer a versatile platform where the absorption bands can be turned over a broad range of wavelengths through control of their shape, size and material properties [14,15].

Exposed to high-power laser illumination, metallic nanostructures can undergo a wide range of NLO responses, including photo-thermal reshaping [16], second harmonic generation [12] and third order optical nonlinearities [17]. Especially interesting are the ordered arrays of plasmonic nanostructures, where the plasmon coupling effect can significantly increase local energy concentration [18-21] compare to the single metal nanostructure. For the ordered metal nanostructures the more efficient optical nonlinearities were observed when the fundamental wavelength of probing light was at plasmonic resonance of the structure [22]. Attention has been paid to the construction of metal nanostructures with specific shapes and lock of symmetry, where the second order nonlinearities can be expected [23]. It was also observed

* Corresponding author. Baumit, Spol. S.r.o., 250 01, Brandýs Nad Labem, Czech Republic.
E-mail addresses: svandaj@post.cz, j.svanda@baumit.cz (J. Švanda).

https://doi.org/10.1016/j.optmat.2020.110695
Received 9 August 2020; Received in revised form 20 November 2020; Accepted 28 November 2020
Available online 23 December 2020

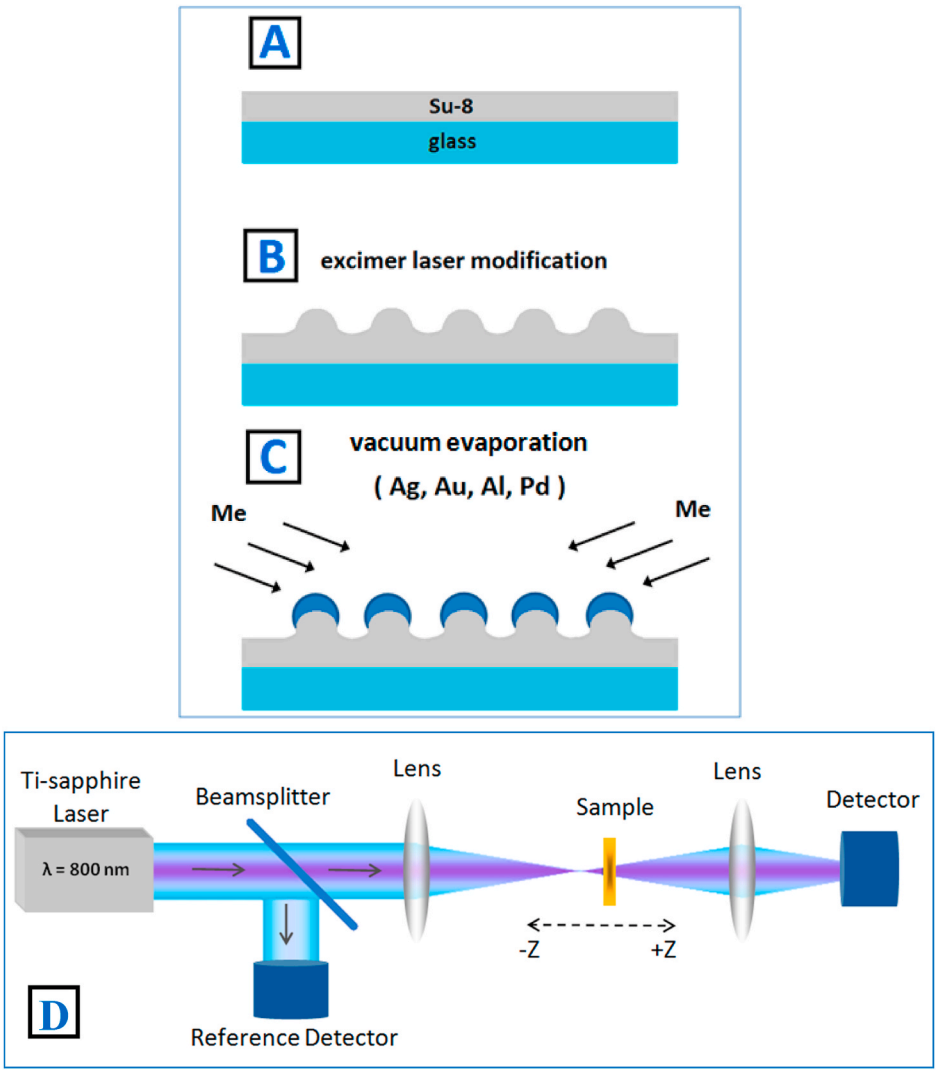

Fig. 1. Schematic representation of the c-shaped metal structures preparation, their characterization, and Z-scan measurements (for more details see the text).

that the traditional rules for symmetry do not play a role in the case of plasmonic structures and the small deviation from an ideal symmetry can lead to the second order nonlinearity appearance [24].

It could be expected, that the combination of plasmonics with nonlinear optics may lead to the construction of a wide range optical components and devices with expected properties and functionalities, including subdiffraction optical microscopy [25], creation of nanolasers logical gates [24], optical modulators [25], all-optical signal processing [2,28,29] and so on [30,31].

In this work we investigate the NLO properties of Ag, Au, Al, Pd highly oriented c-shaped nano-resonator array using the Z-scan technique. The metal nano-resonators were created on the layer of highly resistant, optically transparent and crosslinked resins using excimer laser followed by tilted evaporation of the metals. The creation of proposed structures was confirmed by the conductive AFM and FIB-SEM techniques. The UV–Vis spectra of the prepared structures showed the surface plasmon polariton (SPP) related absorption in the spectral range near the wavelength of probing laser light. This phenomenon, observed using in the Z-scan technique, was crucial for the two photon absorption observation.

2. Experimental

2.1. Materials and samples preparation

A solution of Su-8 - epoxy based photoresist (purchased from Microchem) was spin-coated (1000 rpm, 30 min) onto glass substrates (supplied by Glassbel Ltd., CR) to form polymer films. The samples were dried at 50 °C for 2 h and exposed to a UV-source for 30 min. After that, the samples were dried at 60 °C for 24 h (see Fig. 1).

The polymer surface was patterned by a KrF excimer laser (COMPexPro 50F, Coherent, Inc., wavelength 248 nm, pulse duration 20–40 ns, repetition rate 10 Hz). The laser light was linearly polarized with a UV-grade fused silica cube with an active polarization layer (Fig. 1). The angle of laser beam incidence was 50° with respect to normal to the sample surface. An aperture with an area of 5×10 mm^2 was used. Periodic structures (ripples) on the surface were produced by irradiation with 9000 pulses and fluence of 9 mJ cm^{-1}.

The patterned samples were coated with metals by vacuum evaporation on a Leybold-Heraeus Univex 450 device (room temperature, pressure of 3×10^{-4} Pa). The deposition was performed under angle of 50° with respect to the sample surface normal from both sides to create metallic nano-wires. Ag and Au were evaporated using electrical resistance heating and Al and Pd by the electron gun evaporation. The thickness of all layers was set to be about 20 nm in each step. Scratch test

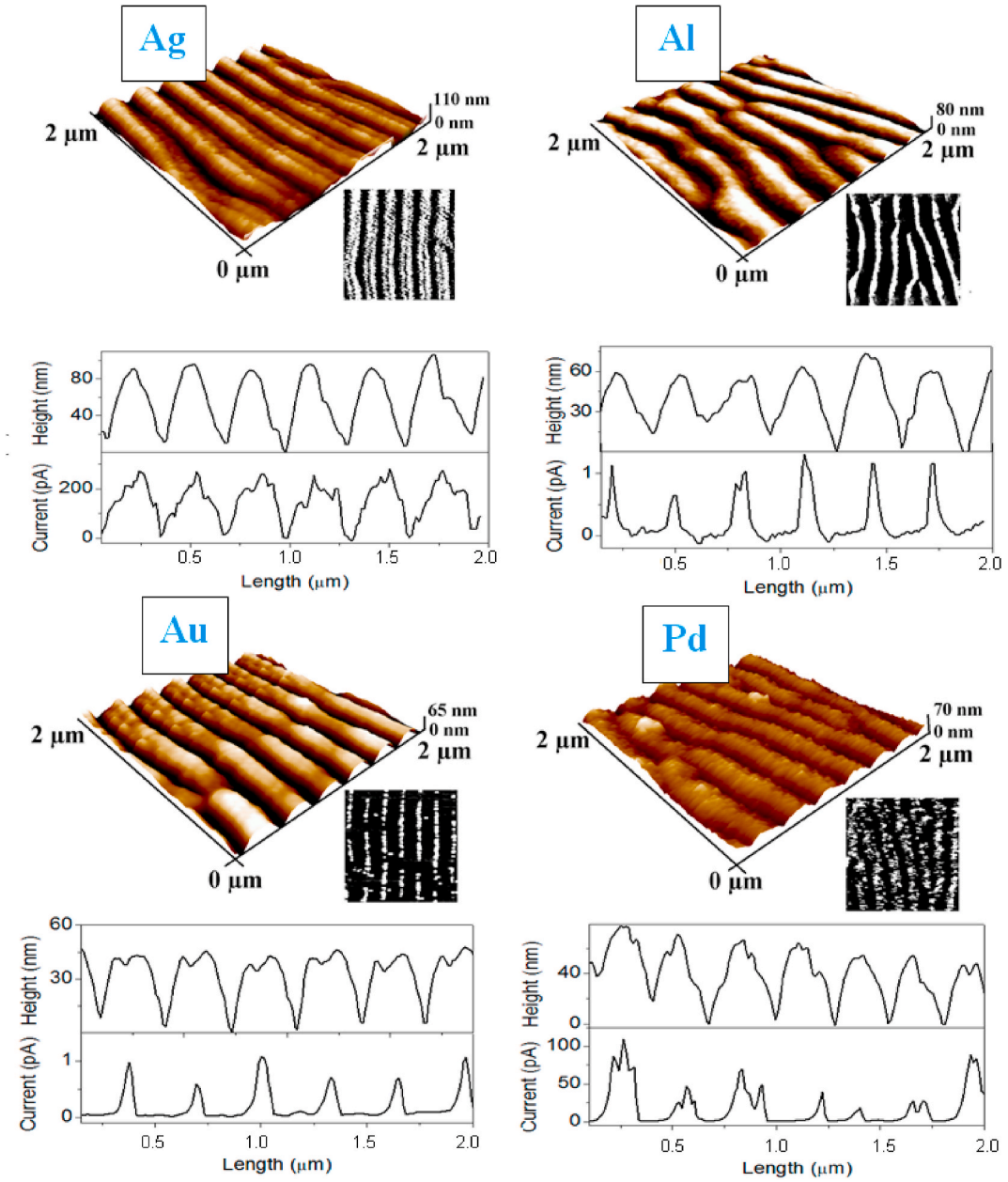

Fig. 2. 2D and 3D morphological AFM scans of the ordered metals nanostructures prepared by the tilted angle metals deposition. Graphs below show the comparison of morphological and conductive cuts for all structures.

was performed by a reference comparative method on the flat glass surface and recalculations of the two-photon absorption on the real thickness were made using the equation mentioned in section 3.4.3.

2.2. Measurement techniques

Linear optical properties were studied using a PerkinElmer Lambda 25 UV/Vis/NIR spectrometer equipped with a wire-grid polarizer (WP25L-UB,Thorlabs) working at spectral range from 250 to 4000 nm. The absorption spectra were recorded in the spectra range from 300 to 1100 nm at scanning rate of 120 nm min^{-1} and a data collection interval of 1 nm.

The surface morphology of the samples was examined using AFM (Icon-Bruker), working in Peak Force mode with Scan-Asyst probe. Conductive AFM measurements were performed with 3 V bias voltage, applied between the sample surface (after silver deposition) and AFM Pt/Pd covered probe. For visual representation of the samples the Focus Ion Beam Scanning Electron Microscope (FIB-SEM, LYRA3 GMU, Tescan, Czech Republic) was used. The FIB cuts were made with a gallium ion beam. The images were taken under the applied voltage of 10 kV.

NLO properties were examined by the open aperture Z-scan technique using a Ti:sapphire amplifier generating 30 fs pulses with a central wavelength at 800 nm and repetition rate of 1 kHz. The laser beam was focused using a 250 mm focal length lens leading to a beam waist radius of 23 µm.

3. Results and discussion

3.1. Ordered c-shaped metal array

Scheme of the preparation of surface plasmon polariton (SPP) supported grating and its non-linear optical characterization is presented in Fig. 1. The flat Su-8 film was deposited by spin-coating (Fig. 1A),

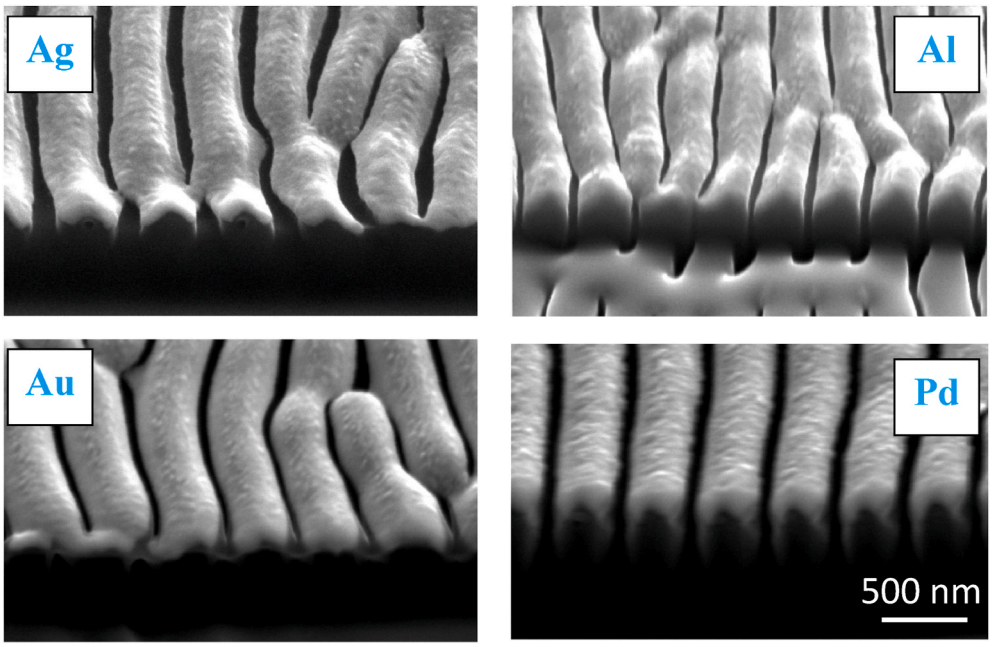

Fig. 3. FIB-SEM image of metals distribution after tilted angle evaporation on the structured polymer surface.

patterned by excimer laser (Fig. 1B) and finally metal-coated by shadow evaporation (Fig. 1C). The created structure represents array of the c-shaped metal nanostructures, which are not connected physically but can efficiently interact with each other. For characterization of its nonlinear optical properties the Z-scan technique was applied (Fig. 1D).

Creation of the periodical structure and results of tilted metal deposition were checked using morphological and conductive AFM techniques. Fig. 2 shows the 3D morphological scans of Su-8 gratings after the metals deposition and corresponding distribution of the surface current. The comparisons of surface profile cutaways with current cutaways are given below the corresponding AFM images. Morphological scans show the well-ordered grating structure and the conductive images represent the well separated conductive and dielectric areas too. Comparison of morphological features with the current pattern indicates the good correlation between surface and current maxima. So, the deposition of metal on the surface tops is clearly visible, confirming the success of a shadow effect which is the basic prerequisite for the creation of ordered c-shaped structure (Fig. 1B).

Further characterization of the shape of the evaporated metal nanostructures was performed using the FIB-SEM technique (see Fig. 3). This technique involves the structure cut-off by the Ga ions beam and further SEM imaging under an inclination with respect to the sample surface. The white areas in Fig. 3, attributed to the conductive material, characterize the metal covering. Arrays of created c-shaped nanostructures are perfectly visible in the case of Ag and Pd. For Al and Au the structure is slightly smeared, but the creation of c-shaped nanostructures is also visible. It should be also noted that the Al structures undergo the quick oxidation at the air, which could explain the slight disagreement between the FIB-SEM and AFM measurements since both these methods are affected by the thin Al oxide layers. However, the optical measurements should not be influenced by this phenomenon within several weeks from the date of the preparation [32]. All these measurements and obtained data confirmed that the preparation of the required structures, as shown in Fig. 1, was successful.

3.2. Linear plasmonic response

The created ordered arrays of c-shaped metal nanostructures are expected to support strongly the excitation and propagation of SPP waves. To characterize the linear optical response of the structure, the

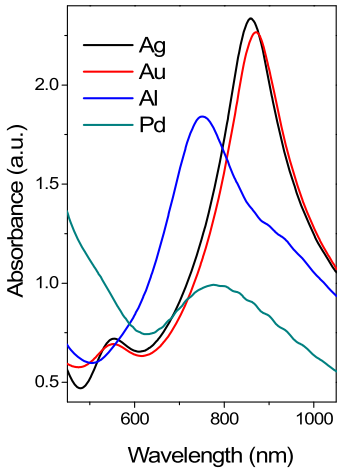

Fig. 4. Absorption spectra (linear absorption) of c-shaped ordered metals nano-array.

UV–Vis measurements were performed and the results are presented in Fig. 4. As could be expected, the prepared structures exhibit the strong SPP absorption band and its peak absorption depends on the metal used. The SPP peak is located at the 870, 850, 780 and 750 nm for Au, Ag, Pd, and, Al respectively. The pronounced and sharp peaks were observed in the case of Ag and Au. The SPP absorption bands of Al and Pd, however, are smeared slightly compared to Ag and Au. It must also be noted that the appearance of SPP related absorption peak is a pronounced function of the light polarization. All spectra presented in Fig. 4 were measured with the light polarization perpendicular to the grating orientation. When the light electric field was oriented along the metal nanostructures the absorption band was not detected. This phenomenon is strongly related to the typical plasmon nature, in which the periodical boundary conditions are required for SPP excitation.

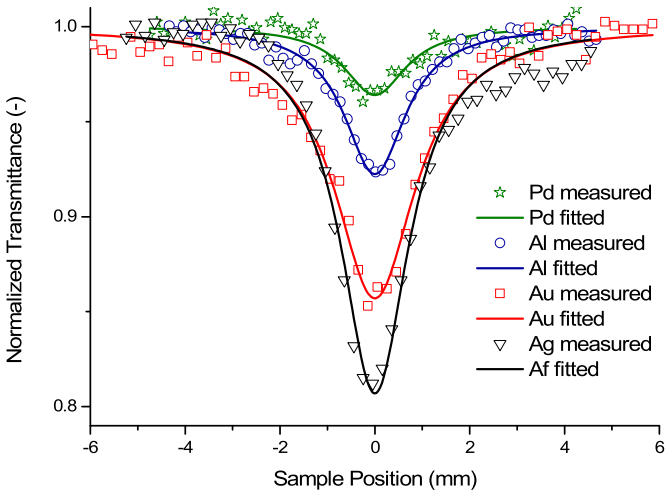

Fig. 5. Experimental results of Z-scans from c-shaped ordered metals nanoarray (points) and corresponding theoretical fit (line).

3.3. Plasmon optical nonlinearity – preliminary experiments

3.3.1. Z-scan technique

The evaluation of the two-photon absorption (2 PA) coefficient was accomplished using Z-scan technique in an open aperture arrangement [33]. The method utilizes a focused Gaussian laser beam of high intensity to trigger the nonlinear optical effects in the sample. Normalized transmittance as a function of the sample position is collected in the course of the sample moving through the focal point of the beam. Determination of the 2 PA coefficient may be complicated by other nonlinear effects since the Z-scan is not able to distinguish between different nonlinearity contributing to the nonlinear absorption. Therefore, the careful determination of experimental data and their exact comparison with a numerical model was necessary. In addition the 2 PA coefficient is a macroscopic material parameter which depends on the light wavelength, pulse duration, repetition rate, concentration of absorbing molecules and dielectric surrounding.

3.3.2. Elimination of polymer/glass response

The prepared SPP supported plasmonic structures were subjected to Z-scan measurements and the results are presented in Fig. 5. To precisely characterize the structure response, a series of experiments were performed on the polymer grating without the metal layer to determine the intensity threshold at which the polymer itself (including the glass substrate) starts to exhibit the nonlinear absorption. Then, the plasmonic-related nonlinearities on the prepared structures were probed with the light intensity substantially smaller than the detected threshold to eliminate the nonlinear absorption contributions of polymer/substrate and assess the absolute metal nanostructures response. Additionally, the possible structure damage was checked using the confocal microscopy and no destructive changes were detected under the applied experimental conditions.

3.3.3. Elimination of thin flat metal response

Further investigation was performed with the aim of eliminating the response of continuous thin metal films, where the plasmon boundary conditions are not satisfied and SPP could not be excited. Experiments were performed at the laser intensity determined in the previous section. Since no nonlinearities were detected in the case of flat metal films all further measured effects can be attributed only to the plasmon response of the prepared metal nanostructure but not to the metal intrinsic properties.

3.4. Plasmon optical nonlinearity – direct experiments

3.4.1. Polarization dependences

Two probing polarization were used to measure the nonlinear optical response of the ordered metal arrays. In the first one electric vector was oriented along the main axes of the metal nanostructures. Since the length of each metal structure can be considered as infinite (i.e. too long in comparison with light wavelength used in Z-scan), the given structure can be considered as having no spatial or translation-symmetric potential, which affects the periodical light-induced oscillation of the free electron gas in metallic nanostructures. In other words, the structure did not show any plasmon behavior and its response to the high light intensity was governed by the intrinsic metal properties. As can be expected, no optical nonlinearity was measured under this polarization. Quite different results were obtained using the light polarization with electric field vector orientation perpendicular to the metal nanostructures main axes. In this case the pronounced effect of transmitted light intensity on the material transparency was detected. It must be additionally noted that in this case the effective plasmon excitation took place (Fig. 4).

3.4.2. Measured curves dependences – two-photon absorption

The normalized transmittance as a function of sample position measured with respect to the focal point of the focused laser beam is shown in Fig. 5. It is evident that all plasmon-supported nanostructures exhibit an apparent optical nonlinearity. Moreover, preliminary experiments at different light polarization clearly show that the observed phenomena solely arise from the plasmonic properties of ordered metal nanostructure. It is also evident that the degree of nonlinearity strongly depends on the strength of the linear plasmonic band. The higher impact of nonlinearity was observed in the case of Ag and Au nanostructures, which also show pronounced absorption bands (see Fig. 4). In the case of Al, the lower intensity of plasmonic band was observed (Fig. 4) which in turn results in the less pronounced plasmon-related nonlinear optical response. The weaker nonlinear response was also detected in the case of Pd nanostructures, which do not exhibit well centered plasmonic band too.

In the next step the careful analysis of the results from the Z-scans, presented in Fig. 5, was performed. Simultaneous absorption of two photons with 800 nm wavelengths corresponds to interband electron transition which can take place in the metals but usually results in only weak absorption peak. So that, the following mechanism of optical nonlinearity can be proposed: under the intensive plasmon excitation a change in the electron intrinsic density distribution occurs, leading to an intensification of electron interband transition, appearance of additional absorption peak and pronounced nonlinear optical response. It should be noted that the observed phenomenon takes place only in the case of metal arrangement in the form of plasmon-supporting nanostructures and was not found in the case of flat metal films, which does not exhibit pronounced plasmon resonance (similar phenomenon was reported for example in papers [2,34–37]).

3.4.3. Optical nonlinearity calculation and fit of experimental data

Known mechanism of optical nonlinearity allows the semi-quantitative estimation of material nonlinearity. For the calculation of two-photon absorption coefficient the following equation was used:

$$T_{(z)} = 1 - \frac{\beta \times I_0 \times L}{2 \times \sqrt{2} \times \left[1 + \left(\frac{z}{z_0}\right)^2\right]} \quad (1)$$

where the $T_{(z)}$ is normalized transmittance, β is two-photon absorption coefficient, I_0 is on-axis light intensity at focal point, L is the metal thickness, and z is the sample position. The model is valid whenever, $0 < \beta \times I_0 \times L < 1$, which is satisfied in the present case and for all metal thicknesses. An effective metal thickness L as an average thickness of the

Table 1
Parameters used for fitting procedure and calculated values of two-photon absorption coefficients β.

Metal	q (−)	I_0 (GW/cm^2)	β (cm/GW)	L (nm)
Au	0,51	$2{,}27\cdot10^{2}$	$1{,}08\cdot10^{3}$	20,96
Ag	0,75	$2{,}64\cdot10^{2}$	$1{,}16\cdot10^{3}$	24,81
Al	0,25	$3{,}77\cdot10^{2}$	$2{,}88\cdot10^{2}$	22,84
Pd	0,11	$4{,}53\cdot10^{2}$	$7{,}15\cdot10^{1}$	33,29

c-shaped metal nanostructures was used for the calculation. The only adjustable parameter in the fitting procedure was coefficient of two-photon absorption β and the results of the best fits are shown in Fig. 5. The extracted values of two-photon absorption coefficient for the investigated metals are presented in Table 1. While the coefficient of two-photon absorption of Ag and Au are high and the same order of magnitude, those for Al and Pd are one or two orders of magnitude lower. As it can be seen from Table 1, the lower values of intensity in case of Ag and Au are sufficient to observe 2 PA represented by q coefficient, which is expressed by the equation: $q < \beta \times I_0 \times L$. Because of the higher q coefficients values, the dips in Fig. 5 are more pronounced. Less 2 PA active material needs to be probed by a laser intensity, which can reach the laser threshold limit, to get the same q coefficient value. The threshold limit was probably reached for Al and Pd during several measurements at the same point, since intensity was around twice as high as for Ag and Au. Q coefficients in both cases decreased, which could be explained by melting of the nanostructures and losing plasmonic properties. To verify this idea, the surfaces were investigated using AFM, but with no results that would confirm it.

Table 2
Comparison of the measured and calculated SPR-related two-photon absorption coefficients with literature data.

Plasmon structure	Probing wavelength (nm)	Experimental details (pulse duration, frequency, intensity)	Resonance wavelength (nm)	Two photon absorption coefficient (cm/GW)	Reference
Ag nanowires in glass	780	130 fs, 76 MHz 1.9 GW/cm^2	720	0.82	[34]
Ag nanoflowers microrods nanowires in suspension	800	87 fs, 1 kHz 399 GW/cm^2 33 GW/cm^2 333 GW/cm^2	400–1100 400 400, 600	$1.54\cdot10^{-2}$ $3.67\cdot10^{-2}$ $1.41\cdot10^{-2}$	[42]
Ag nanorods in borosilicate glass	800	240 fs 800 KHz 8.8 GW/cm^2	400	1.73	[38]
Ag NPs in PVA film	532	5 ns 10 Hz	410	$1.23\cdot10^{-6}$	[43]
Ag NPs with betacyanin dye in PVAC film	532	7 ns 10 Hz 0.4 GW/cm^2	550	$6.88\cdot10^{2}$	[35]
Ag NPs in PMMA film	532		445	$4.04\cdot10^{3}$	[44]
Ag NPs in PVA film	532	CW 2.3 kW/cm^2	421	$2.93\cdot10^{6}$	[45]
Monodispersed Ag NPs in film	1064 532	25 ps 20 Hz 19·09 GW/cm^2 (1064 nm)	490	$4.40\cdot10^{2}$ (1064) $-3.00\cdot10^{4}$ (532)	[39]
Ag ellipsoidal NPs in silicate glass	800	100 fs, 1 KHz 250–350 GW/cm^2	390 450 550 1200	2.20 2.90 $-1.10\cdot10^{3}$ $-6.70\cdot10^{2}$	[46]
Ag NPs in glass	800	200 fs 76 MHz 2.35 GW/cm^2	400	$-1.90\cdot10^{4}$	[47]
Ag nanocubes in DMF	720–920	130 fs 76 MHz 0.25 GW/cm^2	460 490 680	≈≤ 0.00 ≈-3.00 ≈-1.50	[40]
Ag nanostructures	1064	10 ns 0.5 GW/cm^2	435	4.21–6.73	[48]
Au ellipsoidal NPs in bismuthate glass	800	200 fs 76 MHz 1.42 GW/cm^2	865	7.40	[49]
Au triangular nanoprisms in water	1100–1300	200 fs, 76 MHz 0.43 GW/cm^2	1240	$1.89\cdot10^{-1}$	[39]
Au nanocubes and and octahedra NPs in toluene	800	60 fs, 1 KHz 33.1 GW/cm^2	538 552	$1.61\cdot10^{-10}$ $2.44\cdot10^{-10}$	[50]
Au nanorods in PVA film	800	3 ns 10 Hz 8.8 GW/cm^2	≈890	$-7.23\cdot10^{3}$	[51]
Au–Ni–Au nanorods in anodic aluminum oxide	800	0.13 GW/cm^2	800	$-2.65\cdot10^{6}$	[37]
Au metamaterial	890	115 fs 80 MHz 2.3 GW/cm^2	890	$7.70\cdot10^{5}$	[2]
Pd NPs in ethanol	532	4 ns 2 Hz $7.96\cdot10^{-2}$ GW/cm^2		$7.10\cdot10^{1}$	[52]

3.4.4. Comparison with literature data

Careful literature analysis indicates that the plasmon-based 2 PA coefficient has been found to be a function of many parameters, including the noble metal kind, nanostructure morphology and parameters of used laser. For the sake of comparison the values of 2 PA coefficients, measured on the range of precisely engineered plasmonic nanostructures, were collected from the literature and summarized in Table 2. The structures having the plasmon resonance on the wavelength of the laser or its half exhibit the relatively high values of the 2 PA coefficients due to the enhancement of third order nonlinearity or two-photon absorption that is purely originating from the surface plasmon resonance [38]. This is the case of metamaterials, for which demanding preparation and proper design are necessary [2]. The negative values[39,40] of 2 PA coefficients in the fs-regime are probably a consequence of saturable absorption resulting from the fact that the probe wavelength is too far from the resonance wavelength or not twice the resonance wavelength. The experiments with nanoseconds, picoseconds or MHz pulsed lasers cannot be quantitatively compared with present ones since their results are of different nature because of the effects of nonlinearities containing thermal cumulative effects and nonlinear scattering [41]. Comparison of available literature data (Table 2) with the present results indicates that in our case one of the highest values of 2 PA were obtained. It should be noted that most of the results presented in Table 2 are related to the localized surface plasmon resonance, while in our case the plasmon response originates in the surface plasmon polariton, SPP. Therefore, it can be concluded that in the case of SPP excitation and propagation not less but even higher value of two-photon absorption coefficient can be achieved.

4. Conclusion

Relevant information on 2 PA is crucial for applications of materials with highly nonlinear optical activity in optics, informatics and photonics. In this work the ordered array of c-shaped metal nanostructures was proposed as a material with pronounced non-linear optical response. The large scale ordered array was produced through the excimer laser pattering of polymer surface followed by the tilted metals deposition (Ag, Au, Al and Pd were used). These structures are able to support the excitation and propagation of surface plasmon-polariton wave, which was confirmed by linear optical measurements. Examination of the structure response under the high light intensity indicates that: (i) prepared materials show the high value of two photons absorption coefficient; (ii) nonlinear optical response is strongly related to plasmonic properties of created structures but not to the intrinsic properties of constructed materials; (iii) the degree of optical nonlinearity is a strong function of the linear plasmon absorption band intensity. It should finally be noted that further enhancement of the 2 PA could be potentially reached at arbitrary visible wavelengths by shifting the plasmon resonance position to laser wavelength via changing of grating periodicity.

CRediT authorship contribution statement

J. Švanda: Methodology, Validation, Formal analysis, Investigation, Writing - original draft, Writing - review & editing, Project administration. **Y. Kalachyova:** Investigation, Methodology, Software, Validation, Formal analysis, Investigation, Resources, Writing - original draft. **A. Ajami:** Supervision. **P. Macháč:** Investigation. **J. Siegel:** Writing - original draft, Funding acquisition. **Z. Kolská:** Writing - original draft. **P. Slepička:** Writing - original draft, Funding acquisition. **V. Švorčík:** Conceptualization, Methodology, Resources, Writing - original draft, Visualization, Supervision.

Declaration of competing interest

The authors declare that they have no known competing financial interests or personal relationships that could have appeared to influence the work reported in this paper.

Acknowledgement

This work was supported by the GACR under the project 20-01639S and OP VVV Project NANOTECH ITI II. No. CZ.02.1.01/0.0/0.0/18_069/0010045.

References

[1] D. Cotter, R.J. Manning, K.J. Blow, A.D. Ellis, A.E. Kelly, D. Nesset, I.D. Phillips, A. J. Poustie, D.C. Rogers, Nonlinear optics for high-speed digital information processing, Science 286 (5444) (1999) 1523–1528.
[2] M. Ren, B. Jia, J.-Y. Ou, E. Plum, J. Zhang, K.F. MacDonald, A.E. Nikoalenko, J. Xu, M. Gu, N.I. Zheludev, Nanostructured plasmonic medium for terahertz bandwidth all-optical switching, Adv. Mater. 23 (2011) 5540–5544.
[3] G. Steinmeyer, D.H. Sutter, L. Gallmann, N. Matuschek, U. Keller, Frontiers in ultrashort pulse generation: pushing the limits in linear and nonlinear optics, Science 286 (5444) (1999) 1507–1512.
[4] B. Kulyk, A.P. Kerasidou, L. Soumahoro, C. Moussallem, F. Gohier, P. Frereand, B. Sahraoui, Optimization and diagnostic of nonlinear optical features ofp-conjugated benzodifuran-based derivatives, RSC Adv. 6 (2016) 14439–14447.
[5] B. Kulyk, D. Guichaoua, A. Ayadi, A. El-Ghayoury, B. Sahraoui, Functionalized azo-based iminopyridine rhenium complexes for nonlinear optical performance, Dyes Pigments 145 (2017) 256–262.
[6] P. Gunter, Nonlinear Optical Effects and Material, Springer, 2000.
[7] R.W. Boyd, Nonlinear Optics, Elsevier, 2008.
[8] S.I. Anisimov, B.L. Kapeliovich, T.L. Perelman, Electron emission from metal surfaces exposed to ultrashort laser pulses, Sov. Phys. JETP 39 (2) (1974) 375–377.
[9] Y. Kalachyova, D. Mares, O. Lyutakov, M. Kostejn, L. Lapcak, V. Svorcik, Surface plasmon polaritons on silver gratings for optimal SERS response, J. Phys. Chem. C 119 (17) (2015) 9506–9512.
[10] J. Svanda, Y. Kalachyova, P. Slepicka, V. Svorcik, O. Lyutakov, Smart component for switching of plasmon resonance by external electric field, ACS Appl. Mater. Interfaces 8 (1) (2016) 225–231.
[11] C. Ciracì, R.T. Hill, J.J. Mock, Y. Urzhumov, A.I. Fernández-Domínguez, S. A. Maier, J.B. Pendry, A. Chilkoti, D.R. Smith, Probing the ultimate limits of plasmonic enhancement, Science 337 (2012) 1072–1074.
[12] M. Kauranen, A.V. Zayats, Nonlinear plasmonics, Nat. Photon. 6 (2012) 737–748.
[13] J. Butet, P.-F. Brevet, O.J.F. Martin, Optical second harmonic generation in plasmonic nanostructures: from fundamental principles to advanced applications, ACS Nano 9 (2015) 10545–10562.
[14] W. Li, C. Ma, L. Zhang, B. Chen, L. Chen, H. Zeng, Tuning localized surface plasmon resonance of nanoporous gold with a silica shell for surface enhanced Raman scattering, Nanomaterials 9 (251) (2019) 1–7.
[15] K. Gambhir, B. Ray, R. Mehrotra, P. Sharma, Morphology dependent two photon absorption in plasmonic structures and plasmonic–organic hybrids, Optic Laser. Technol. 90 (2017) 201–210.
[16] S. Link, C. Burda, B. Nikoobakht, M.A. El-Sayed, Laser-induced shape changes of colloidal gold nanorods using femtosecond and nanosecond laser pulses, J. Phys. Chem. B 104 (26) (2000) 6152–6163.
[17] Y. Yu, Y. Bao, L. Lin, H. Xu, R. Liu, Z. Zhou, Large third-order optical nonlinearity and ultrafast optical response in thin Au nanodiscs, Opt. Mater. Express 9 (7) (2019) 3021–3034.
[18] Y. Kalachyova, D. Mares, V. Jerabek, K. Zaruba, P. Ulbrich, L. Lapcak, V. Svorcik, O. Lyutakov, The effect of silver grating and nanoparticles grafting for LSP-SPP coupling and SERS response intensification, J. Phys. Chem. C 120 (19) (2016) 10569–10577.
[19] P.V. Kamat, J. Meeting the clean energy Demand: nanostructure architectures for solar energy conversion, Phys. Chem. C 111 (7) (2007) 2834–2860.
[20] O. Guselnikova, Y. Kalachyova, K. Hrobonova, M. Trusova, J. Barek, P. Postnikov, V. Svorcik, O. Lyutakov, SERS platform for detection of lipids and disease markers prepared using modification of plasmonic-active gold gratings by lipophilic moieties, Sens. Actuat. B: Chem. 265 (2018) 182–192.
[21] Y. Kalachyova, O. Guselnikova, R. Elashnikov, I. Panov, J. Žádný, V. Církva, J. Storch, J. Sykora, K. Zaruba, V. Svorcik, O. Lyutakov, Helicene-SPP-based chiral plasmonic hybrid structure: toward direct enantiomers SERS discrimination, ACS Appl. Mater. Interfaces 11 (1) (2019) 1555–1562.
[22] H. Tuovinen, M. Kauranen, K. Jefimovs, P. Vahimaa, T. Vallius, J. Turunen, N. V. Tkachenko, H. Lemmetyinen, Linear and second-order nonlinear optical properties of arrays of noncentrosymmetric gold nanoparticles, J. Nonlinear Opt. Phys. Mater. 11 (4) (2002) 421–432.
[23] B. Lamprecht, A. Leitner, F.R. Aussenegg, Femtosecond decay-time measurement of electron-plasma oscillation in nanolithographically designed silver particles, Appl. Phys. B 64 (1997) 269–272.
[24] B.K. Canfield, S. Kujala, K. Jefimovs, J. Turunen, M. Kauranen, Linear and nonlinear optical responses influenced by broken symmetry in an array of gold nanoparticles, Optic Express 12 (2004) 5418–5423.
[25] G. Deka, C.K. Sun, K. Fujita, K.S.W. Chu, Nonlinear plasmonic imaging techniques and their biological applications, Nanophotonics 6 (1) (2017) 31–49.
[28] S. Bashiri, K. Fasihi, An all-optical 1× 2 demultiplexer using Kerr nonlinear nano-plasmonic switches, Plasmonics 15 (2020) 449–456.

[29] Y. Liu, G. Bartal, D.A. Genov, X. Zhang, Subwavelength discrete solitons in nonlinear metamaterials, Phys. Rev. Lett. 99 (2007) 153901.
[30] S. Sederberg, C.J. Firby, S.R. Greig, A.Y. Elezzabi, Integrated nanoplasmonic waveguides for magnetic, nonlinear, and strong-field devices, Nanophotonics 6 (1) (2017) 235–257.
[31] S. Gwo, C.K. Shih, Semiconductor plasmonic nanolasers: current status and perspectives, Rep. Prog. Phys. 79 (8) (2016) 86501.
[32] M.W. Knight, N.S. King, L. Liu, H.O. Everitt, P. Nordlander, N.J. Halas, Aluminum for plasmonics, ACS Nano 8 (1) (2014) 834–840.
[33] P.B. Chapple, J. Staromlynska, J.A. Hermann, T.J. Mckay, Single-beam Z-scan: measurement technique and analysis, J. Nonlinear Opt. Phys. Mater. 6 (3) (1997) 251–293.
[34] Q.Q. Wang, J.B. Han, H.M. Gong, D.J. Chen, X.J. Zhao, J.Y. Feng, J.J. Ren, Linear and nonlinear optical properties of Ag nanowire polarizing glass, Adv. Funct. Mater. 16 (2006) 2405–2408.
[35] A. Sarkar, A. Thankappan, V.P.N. Nampoori, Effect of silver nanoparticles on fluorescence and nonlinear properties of naturally occurring betacyanin dye, Opt. Mater. 39 (2015) 211–217.
[36] Z. Chen, H. Dai, J. Liu, H. Xu, Z. Li, Z.K. Zhou, J.B. Han, Dipole plasmon resonance induced large third order optical nonlinearity of Au triangular nanoprism in infrared region, Optic Express 21 (15) (2013) 17568–17575.
[37] Y. Yu, S.S. Fan, X. Wang, Z.W. Ma, H.W. Dai, J. Han, Large third-order optical nonlinearity in coupled Au–Ni–Au composite nanorods, Mater. Lett. 134 (2014) 233–236.
[38] M. Kyoung, M. Lee, Nonlinear absorption and refractive index measurements of silver nanorods by the Z-scan technique, Optic Commun. 171 (1999) 145–148.
[39] P. Lama, A. Suslov, A.D. Walser, R. Dorsinville, Plasmon assisted enhanced nonlinear refraction of monodispersed silver nanoparticles and their tenability, Optic Express 22 (11) (2014) 14014–14021.
[40] K. Zhang, Z.L. Huang, H.W. Dai, Z.W. Ma, J.B. Han, H.M. Gong, Y.B. Han, Surface plasmon enhanced third-order optical nonlinearity of silver nanocubes, Opt. Mater. Express 5 (11) (2015) 2645–2654.
[41] J. Olesiak-Banska, M. Gordel, R. Kolkowski, K. Matczyszyn, M. Samoc, Third-order nonlinear optical properties of colloidal gold nanorods, J. Phys. Chem. C 116 (2012) 13731–13737.
[42] S. Luo, Y. Chen, G. Fan, F. Sun, S. Qu, Saturable absorption and reverse saturable absorption on silver particles with different shapes, Appl. Phys. A 177 (2) (2014) 891–894.
[43] V. Singh, P. Aghamkar, Surface plasmon enhanced third-order optical nonlinearity of Ag nanocomposite film, Appl. Phys. Lett. 104 (2014) 111112.
[44] Y. Sun, Y. Liu, G. Zhao, X. Zhou, Q. Zhang, Y. Deng, Controlled formation of Ag/poly(methyl-methacrylate) thin films by RAFT technique for optical switcher, Mater. Chem. Phys. 111 (2008) 301–304.
[45] M. Ghanipour, D. Dorranian, Nonlinear optical characterization of the Ag nanoparticles in polyvinyl alcohol film, Nonl. Quantum Opt. 118 (6) (2015) 949–954.
[46] S. Mohan, J. Lange, H. Graener, G. Seifert, Surface plasmon assisted optical nonlinearities of uniformly oriented metal nano-ellipsoids in glass, Optic Express 20 (27) (2012) 28655–28663.
[47] L. Karvonen, J. Rönn, S. Kujala, Y. Chen, A. Säynätjoki, A. Tervonen, Y. Svirko, S. Honkanen, High non-resonant third-order optical nonlinearity of Ag–glass nanocomposite fabricated by two-step ion exchange, Opt. Mater. 36 (2013) 328–332.
[48] S. Biswas, A.K. Kole, P. Kumbhakar, Observation of two-photon induced three-photon absorption in chemically synthesized silver nanostructured, Chem. Phys. Lett. 629 (2015) 70–75.
[49] F. Chen, S. Dai, T. Xu, X. Shen, C. Lin, Q. Nie, C. Liu, J. Heo, Surface-plasmon enhanced ultrafast third-order optical nonlinearities in ellipsoidal gold nanoparticles embedded bismuthate glasses, Chem. Phys. Lett. 214(2011) 79–82.
[50] Y.H. Lee, Y. Yan, L. Polavarapu, Q.H. Xu, Nonlinear optical switching behavior of Au nanocubes and nano-octahedra investigated by femtosecond Z-scan measurements, Appl. Phys. Lett. 95 (2009) 23105.
[51] J. Li, S. Liu, Y. Liu, F. Zhou, Z.Y. Li, Anisotropic and enhanced absorptive nonlinearities in macroscopic film induced by aligned gold nanorods, Appl. Phys. Lett. 96 (26) (2010) 263103.
[52] G. Fan, S. Qu, Q. Wang, C. Zhao, L. Zhang, Z. Li, Pd nanoparticles formation by femtosecond laser irradition and the nonlinear optical properties at 532 nm using nanosecond laser pulses, J. Appl. Phys. 109 (2011), 23102 1–8.